



**UNIVERSITY OF LEEDS**

This is a repository copy of *The role of Central Asian uplift in East Asian Monsoon circulation and its palaeoclimate implication*.

White Rose Research Online URL for this paper:  
<http://eprints.whiterose.ac.uk/155693/>

Version: Accepted Version

---

**Article:**

Zoura, D, Haywood, AM [orcid.org/0000-0001-7008-0534](https://orcid.org/0000-0001-7008-0534), Hill, DJ  
[orcid.org/0000-0001-5492-3925](https://orcid.org/0000-0001-5492-3925) et al. (2 more authors) (2020) The role of Central Asian uplift in East Asian Monsoon circulation and its palaeoclimate implication. *Global and Planetary Change*, 184. 103073. ISSN 0921-8181

<https://doi.org/10.1016/j.gloplacha.2019.103073>

---

© 2019, Elsevier B.V. This manuscript version is made available under the CC-BY-NC-ND 4.0 license <http://creativecommons.org/licenses/by-nc-nd/4.0/>.

**Reuse**

This article is distributed under the terms of the Creative Commons Attribution-NonCommercial-NoDerivs (CC BY-NC-ND) licence. This licence only allows you to download this work and share it with others as long as you credit the authors, but you can't change the article in any way or use it commercially. More information and the full terms of the licence here: <https://creativecommons.org/licenses/>

**Takedown**

If you consider content in White Rose Research Online to be in breach of UK law, please notify us by emailing [eprints@whiterose.ac.uk](mailto:eprints@whiterose.ac.uk) including the URL of the record and the reason for the withdrawal request.



[eprints@whiterose.ac.uk](mailto:eprints@whiterose.ac.uk)  
<https://eprints.whiterose.ac.uk/>

1 **The role of Central Asian uplift in East Asian Monsoon circulation and its palaeoclimate**  
2 **implication**

3 D. Zoura<sup>a</sup>, A.M. Haywood<sup>a</sup>, D.J. Hill<sup>a</sup>, A.M. Dolan<sup>a</sup>, Z. Tang<sup>b</sup>,

4 <sup>a</sup>School of Earth and Environment, Woodhouse Lane, University of Leeds, Leeds, LS2 9JT, UK

5 <sup>b</sup>Key Laboratory of Cenozoic Geology and Environment, Institute of Geology and Geophysics, Chinese Academy  
6 of Sciences, Beijing 100029, China

7

8 **Abstract**

9 It has been clearly established that the climate of Asia is significantly affected by high-elevation  
10 orogens such as the Tibetan Plateau, Mongolian Plateau and Tian-Shan. The East Asian Monsoon  
11 (EAM), one of the most prominent features of Asian climate, has been well studied in a modern  
12 context and its dynamics are generally well understood. However, specific features of the EAM are  
13 less studied and understood in a palaeoclimate context, largely because of associated uncertainties in  
14 palaeotopography for the Cenozoic era. Here, we investigate changes in the individual stages of the  
15 EAM in response to increasing topography over Central Asia. We perform a series of sensitivity  
16 experiments with different palaeogeographic elevations using a coupled ocean-atmosphere General  
17 Circulation Model (HadCM3), to investigate seasonal variability of the EAM, and investigate the  
18 emergent critical threshold in elevation where the patterns of atmospheric circulation and climate  
19 over Asia attains the characteristics observed in the modern climate system. Our results indicate that  
20 above an elevation threshold of 3000 m, EAM circulation follows the modern pattern, but below that  
21 threshold, EAM circulation and precipitation follow a distinctly different pattern, where the westerly  
22 jet does not propagate into the higher latitudes and monsoonal precipitation is limited to June and  
23 July. This shift in circulation pattern has important implications for the successful interpretation of  
24 proxy-based palaeoclimate and environmental reconstructions. In addition, our results emphasize the

25 importance of the latitudinal position of high-elevation on the EAM circulation, by showing that low-  
26 elevation can produce modern-like EAM conditions, if located at different latitudes than modern.

27 Keywords: East Asian Monsoon, uplift, climate, monsoonal precipitation

28

## 29 **1. Introduction**

30 The uplift of the Tibetan Plateau (TP) was the most dramatic tectonic event in recent geological history  
31 (X. D. Liu and Dong 2013), and is one of the suggested factors that drove climatic change in Asia during  
32 the Cenozoic (Wu et al. 2007). Geological evidence links TP uplift with the development of the Asian  
33 monsoon and inland aridification (An et al. 2001; Guo et al. 2002). Despite decades of study,  
34 controversy remains over the tectonic history of the continent since the Palaeogene. Although most  
35 studies concur on the existence of an early proto-plateau in the southern margin of Asia, the  
36 palaeolatitude of this feature during the Cenozoic remains unclear (Lippert et al., 2014). Southern  
37 Tibet has remained approximately at its present height for  $35 \pm 5$  Ma (Rowley and Currie 2006), yet  
38 the elevation history of northern Tibet remains only partially constrained (Molnar et al., 2010).  
39 Additionally, geological evidence indicates that the Tian-Shan (TS) orogen and the Mongolian Plateau  
40 (MP) experienced significant uplift since the late Miocene (R. Zhang et al. 2017), and in turn this uplift  
41 caused a decrease in annual precipitation over inland Asia (Liu et al. 2015). The effects of the uplift of  
42 the whole TP have been explored in a number of numerical climate modelling studies since the 1970's  
43 (e.g. Manabe and Terpstra 1974). For example, An et al. (2001) used an Atmospheric General  
44 Circulation Model (AGCM within CCM3) to perform experiments with idealized stages of elevation for  
45 the TP. Liu and Yin (2002) also used an AGCM with more intermediate uplift stages to investigate the  
46 effect of uplift in the evolution of the East Asian Monsoon (EAM). However, it was not until recently  
47 that studies focused on the latitudinal distribution of the TP and not simply its elevation (e.g. Zhang  
48 et al. 2018). The tectonic evolution and uplift of the Tian Shan orogen is not as well studied and  
49 constraint as the Tibetan Plateau. Studies in the past indicate that the uplift of Tian Shan orogen began

50 in the Late Oligocene to Early Miocene (Sobel and Dumitru 1997; Yin et al. 1998). Middle Miocene is  
51 the period that researchers have pointed out as the onset of rapid growth and its being ongoing ever  
52 since (Aitken 2011). However, parts of the Tian Shan comprise of marine sediments and ophiolites  
53 that date back to Cambrian (Brunet et al. 2017).

54 The formation of the Mongolian Plateau has been attributed by some researchers to the collision  
55 between India and Eurasia (i.e. De Grave et al. 2007) while other studies propose that it is a product  
56 of the interaction between a mantle plume and continental lithosphere (i.e. Windley and Allen 1993).  
57 Additionally, Jolivet et al. (2007), showed that the plateau has been uplifted since the Jurassic but did  
58 not attain its current elevation until the Late Miocene.

59 Recent modelling studies using higher resolution GCMs have shown that the uplift of TP, TS and MP  
60 all played an important role for East Asian climate, causing a decrease in precipitation and changes to  
61 low-level and middle-tropospheric winds due to changes in the thermal structure of the atmosphere  
62 (R. Zhang et al. 2017). Modern East Asian climate has been studied extensively, as it influences over 1  
63 billion people and is of particular interest due to its unique characteristics that do not conform with  
64 the behaviour of typical monsoons (Chiang et al. 2014), as the monsoonal precipitation and winds are  
65 associated with frontal systems and the jet stream (Molnar et al., 2010), rather than the tropical  
66 monsoon circulation in which precipitation is primarily linked with the Intertropical Convergence Zone  
67 (ITCZ). Additionally, the south to north migration of the westerly jet during boreal summer over East  
68 Asia plays an important role in driving seasonality and transitions of monsoonal precipitation (Chiang  
69 et al. 2014). The initiation of the EAM has been attributed to a change from a zonal to a non-zonal  
70 monsoon climate pattern (Li et al. 2018), however the timing of the onset and the abrupt changes of  
71 the EAM during past climates, and in turn the mechanisms controlling it, are still under investigation.

72 In this study, we use a fully coupled GCM (HadCM3) to carry out simulations with different topographic  
73 configurations for high-elevation Central Asia. Specifically, starting with the pre-industrial topography,  
74 we decrease the elevation over the area covering the TP, MP and TS in regular stages, resulting in five

75 different intermediate elevation experiments (see section 2.2 for details). We also carry out two  
76 additional simulations with this region set to sea-level and a simulation with Oligocene-like  
77 topography over Asia (after Markwick 2007), in order to assess the climatic response to the latitudinal  
78 distribution of high elevation areas. Focusing on the East Asian monsoon, we explore: a) the seasonal  
79 variability of the westerly jet and associated precipitation over East Asia, b) the elevation threshold  
80 for changes in the climate patterns over Asia and c) the westerly jet latitudinal position in relation to  
81 the uplift to determine the role of high elevation as a palaeoclimate forcing altering the jet.

82

## 83 **2. Methods**

84

### 85 **2.1 Model description and experimental design**

86 For this study, we use the UK Met Office coupled atmosphere-ocean HadCM3 General Circulation  
87 Model (GCM), with the MOSES 1 land-surface scheme (Cox et al. 1999). HadCM3 consists of a  
88 dynamically coupled atmosphere, ocean and sea-ice model (see Gordon et al. 2000 for further details).  
89 The horizontal resolution of the model is  $3.75^\circ \times 2.5^\circ$  for the atmosphere which corresponds to 278  
90 km x 295 km at  $45^\circ$  latitude and 278 x 417 km at the equator and  $1.25^\circ \times 1.25^\circ$  for the ocean, producing  
91 a global grid of 96 x 73 grid cells. The vertical layers for the atmosphere and ocean are 19 and 20  
92 respectively. The orography and gravity wave parameterization include the effects of flow blocking,  
93 trapped lee waves, and high drag states (Gregory et al. 1998; Pope et al. 2000). Precipitation is  
94 produced by the convection scheme and the large-scale precipitation scheme. The large-scale  
95 precipitation and cloud scheme is produced as described in Smith (1990) regarding an explicit cloud  
96 water variable. The majority of the 19 atmospheric layers are distributed in less than 10 km altitude  
97 (13 layers in total), whereas 9 of them are distributed between 0 and 5 km (Pope et al. 2001).  
98 HadCM3 has been used successfully in the representation of modern Asian climate (Jiang et al., 2005)  
99 and can reproduce with success seasonal and annual precipitation.

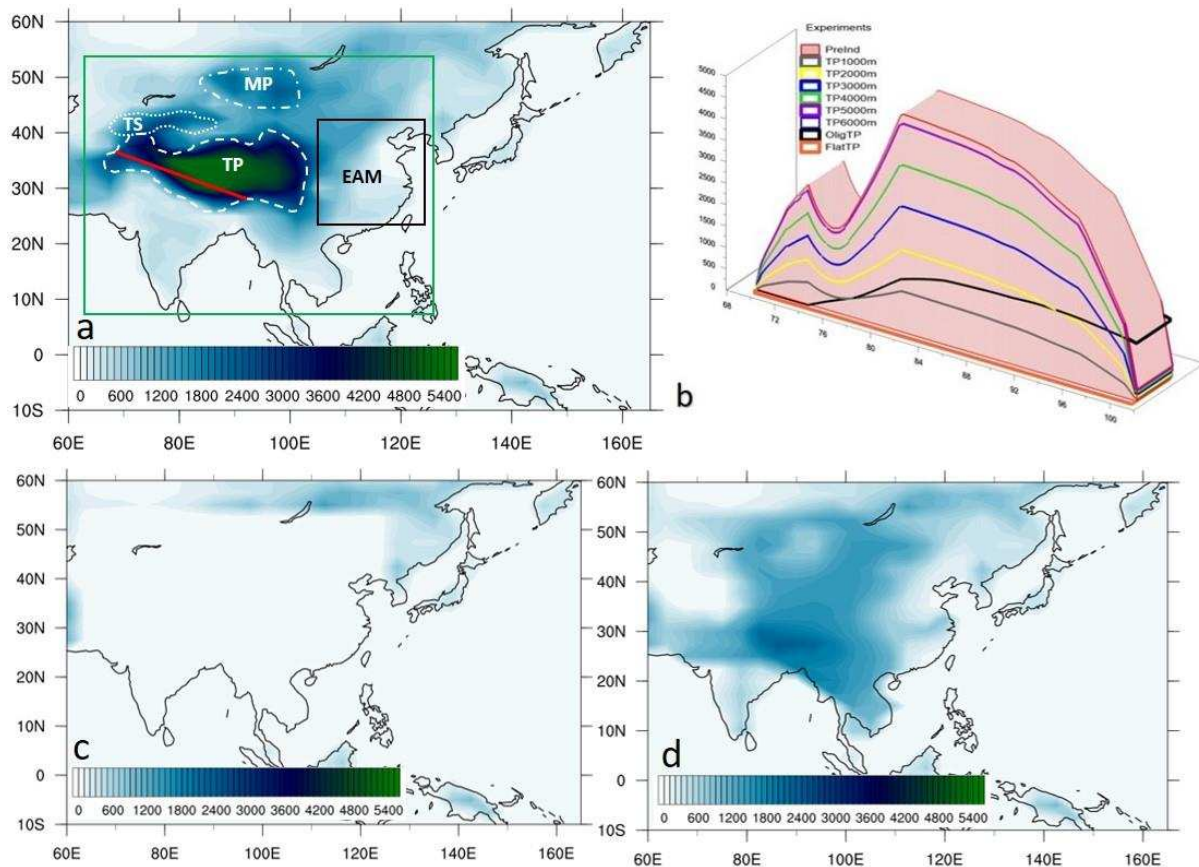
100 In contrast to previous climate modelling studies that have examined the effect only uplifting the TP,  
 101 in this study we uplift all major Central Asian orogens (namely the TP, TS and MP). Specifically, we  
 102 decrease elevations from modern by 96%, 77%, 58%, 38% and 19% (hereafter referred to as TP5000,  
 103 TP4000, TP3000, TP2000 and T1000 respectively). The number following “TP” in the experiment name  
 104 denotes the maximum elevation of the TP in each experiment in metres (Table 1). Additionally, we  
 105 carried out a simulation with no orogens in Central Asia where TP, TS and MP were set to sea-level  
 106 (hereafter referred to as FlatTP). Finally, a simulation with Oligocene-like elevation (OligTP) in Central  
 107 Asia (after Markwick 2007) was completed, where the TS and MP were at elevations lower than 1000  
 108 m (see Fig 1a), and the TP was at approximately 2300 m elevation but was located at a lower latitude  
 109 (Fig.1b). The changing elevation in the model is implemented over the area between 62.5°E and 125°E  
 110 and 20°N – 52.5°N (Fig.1b). All other boundary conditions for each experiment were kept constant and  
 111 specified as pre-industrial (PreInd). Specifically, atmospheric CO<sub>2</sub> was set to 280 ppmv, vegetation type  
 112 and distribution was specified as being modern, as was the land-sea distribution, ice-sheet coverage  
 113 and topography for the rest of the globe, outside of the geographical domain specified above. The  
 114 experiments were not designed to represent a specific geological period of the past, but since the  
 115 influence of the TP, TS and MP are considered predominant for the evolution of East Asian climate  
 116 during the Cenozoic (Zoura et al. 2019), our experimental design represents an appropriate  
 117 methodology to better understand regional uplift and how uplift controlled the way that the East  
 118 Asian climate regime developed. Each simulation was performed for 500 simulated years with the final  
 119 100 years used to derive the required climatological means for subsequent analysis.

| <b>Experiment name</b> | <b>Maximum TP elevation</b> | <b>Maximum MP elevation</b> | <b>Maximum TS elevation</b> |
|------------------------|-----------------------------|-----------------------------|-----------------------------|
| PreInd                 | 5351                        | 2425                        | 4100                        |
| FlatTP                 | sea level                   | sea level                   | sea level                   |
| TP1000                 | 1016.69                     | 460.75                      | 779                         |

|        |         |         |      |
|--------|---------|---------|------|
| TP2000 | 2033.38 | 921.5   | 1558 |
| TP3000 | 3103.58 | 1406.5  | 2378 |
| TP4000 | 4120.27 | 1867.25 | 3157 |
| TP5000 | 5136.96 | 2328    | 3936 |
| OligTP | 2364    | 900     | 1100 |

120

121 Table 1: List of experiments with maximum elevation (metres above sea level) for the Tibetan Plateau (TP), Mongolian  
 122 Plateau (MP) and Tianshan (TS) orogen respectively.



123

124 Fig. 1: a) Pre-industrial (PreInd) elevation. The dashed line shows the Tibetan Plateau (TP), dotted line the Tian-Shan (TS),  
 125 dash/dot line the Mongolian Plateau (MP), black box shows the region used to analyse the East Asian Monsoon (EAM)  
 126 patterns, and the green box the area over which the elevation is decreased for all the experiments (see section 2.2 for  
 127 details); the red line shows the axis along which elevation profiles are shown in b. b) Elevation profiles for the simulations  
 128 carried out by this study along the (red) axis shown in a). c) flattened TP, TS and MP topography d) Oligocene-like elevation  
 129 (after Markwick, 2007).

130

### 131 **3. Results**

#### 132 **3.1 East Asian Monsoon precipitation**

133 The rainfall pattern from April to July over East Asia can be divided in the following four stages: 1)  
134 persistent rainfall in April over the South EAM region, 2) Pre-Meiyu phase in May, 3) Meiyu rainfall in  
135 June where rainfall shifts northward and 4) second northward jump of the rainfall that marks the end  
136 of the Meiyu stage (Chiang et al. 2014; Molnar et al. 2010). The term Meiyu is associated with the  
137 subtropical front that brings summer rainfall over the EAM region and is one of its most prominent  
138 features. For the purpose of this paper, we are studying the East Asian Monsoon from a frontal system  
139 perspective. We include the April rainfall that occurs in the Southern part of the EAM region as it is  
140 associated with convergent frontal circulation (Zhou et al., 2004) and we do not include August as the  
141 Meiyu front is reaching maturity in mid-July and the northward jump during this month is marking the  
142 end of the Meiyu front, making August a post-Meiyu season (Chen and Bordoni, 2014).

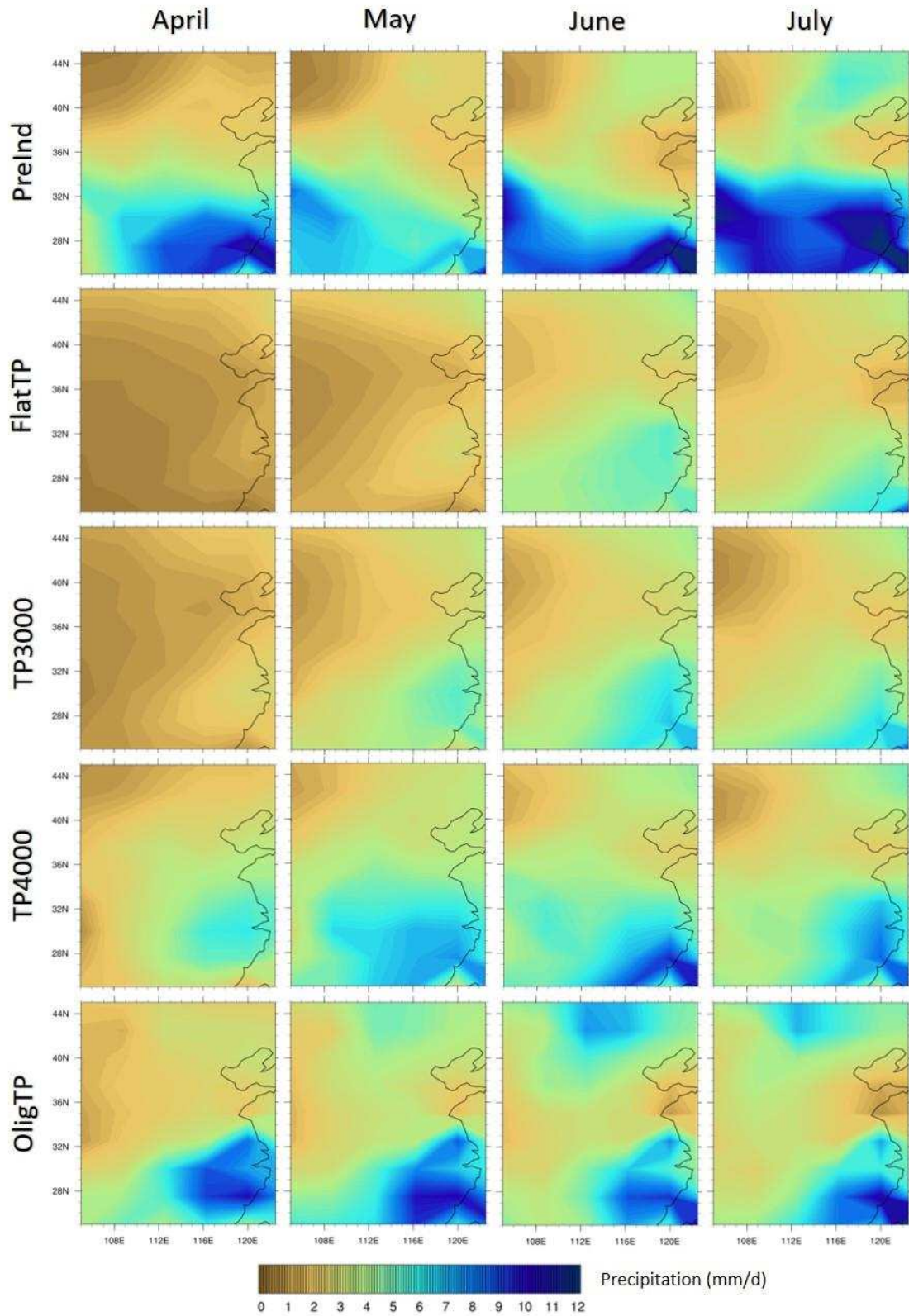
143 With boundary conditions set to PreInd and TP5000, simulated precipitation from April to July follows  
144 the modern-like seasonal variability and spatial extent described above (Fig. 2, S1). Furthermore, our  
145 experiments show that spring rainfall over East Asia is absent with topography set to less than TP2000,  
146 indicating dry conditions during spring (Fig. 2). Greater elevation produces an increase in spring rainfall  
147 South of the Yangtze river (approx. 31°N), characteristic of the first stage of the EAM (Fig. 2). The  
148 tipping point from the dry conditions to the persistent spring rainfall, and thus the formation of stage  
149 1 of the modern EAM, is seen in experiment TP3000. In TP3000, spring precipitation is significantly  
150 decreased in terms of extent and intensity than experiment PreInd, and conditions resemble the  
151 PreInd pattern when elevation surpasses that of TP4000. In the OligTP experiment, spring rainfall over  
152 the south part of the EAM region is close to PreInd in terms of intensity but is more limited spatially  
153 and mainly affecting the southeast EAM (Fig. 2). Interestingly, even though in terms of “absolute”  
154 elevation the OligTP is set to less than that of TP3000, stage 1 of the EAM is not absent.



155 The FlatTP to TP2000 experiments produce dry conditions during the second stage of the EAM (Fig. 2,  
156 S1), and again TP3000 is the threshold elevation for a shift to wetter conditions that can be  
157 characterized as the pre-Meiyu phase, even though limited to the southeast of the region. The OligTP  
158 simulation shows the precipitation zone extending to the west and north, indicative of stage 2 EAM  
159 circulation (Fig. 2).

160 During the Meiyu phase, all experiments show a precipitation increase and northward propagation  
161 (Fig. 2). Lower elevation produces weakened and spatially limited precipitation (i.e. FlatTP), but as we  
162 move to the higher elevation experiments the pattern becomes increasingly similar to the PreInd.

163 Finally, in July rainfall propagation into the higher latitudes is evident in experiments TP3000 or above  
164 even though weaker compared to the PreInd (Fig. 2). This is not the case for the FlatTP simulation  
165 where precipitation is spatially confined to the lower latitudes. The OligTP experiment shows a  
166 relatively dry zone over the central EAM region, however the South and North are significantly wetter  
167 (Fig. 2).



168

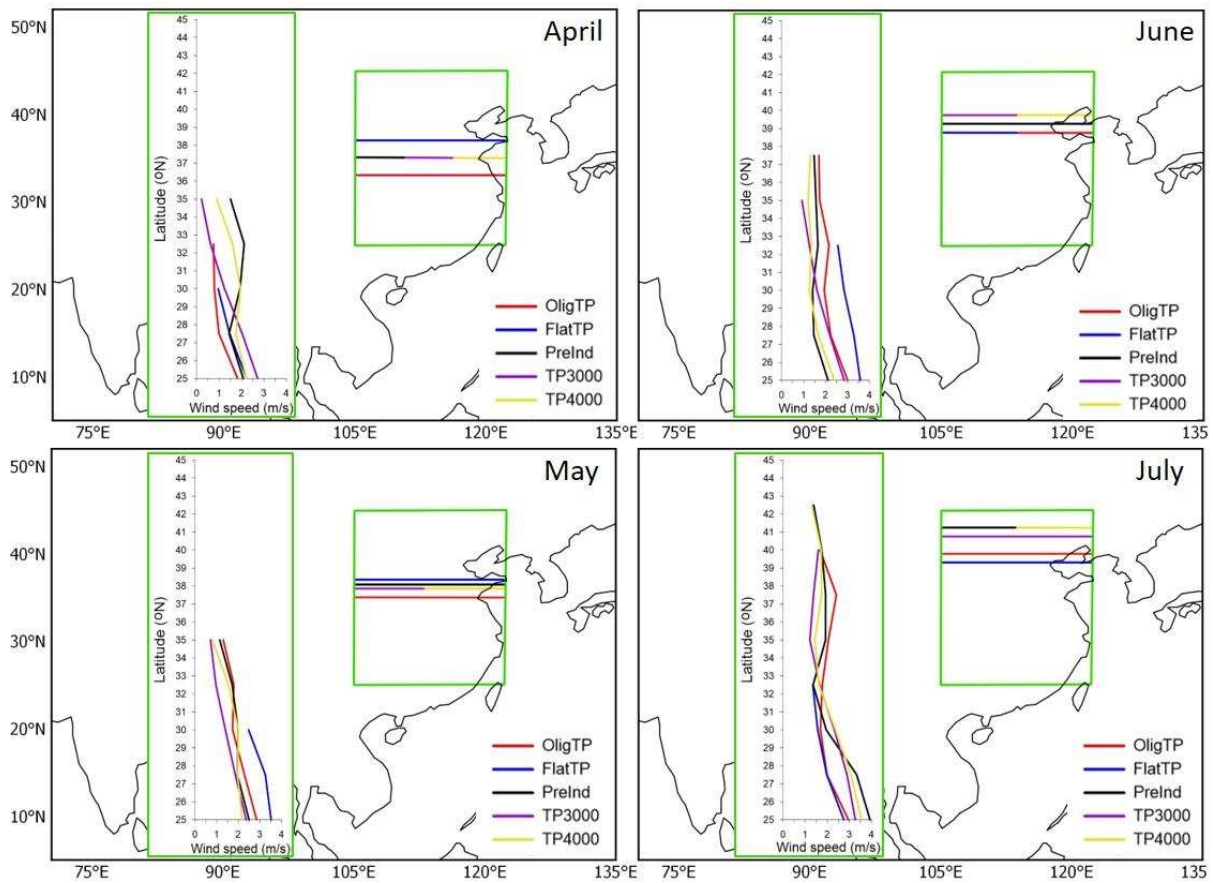
169

170 Fig. 2: April to July monthly total precipitation rate (mm/day). Experiments TP1000, TP2000 and TP5000 are shown in the  
 171 Supplementary.

172  
173  
174  
175  
176  
177  
178  
179  
180  
181  
182  
183  
184  
185  
186

**3.2 Westerly jet and meridional temperature gradient**

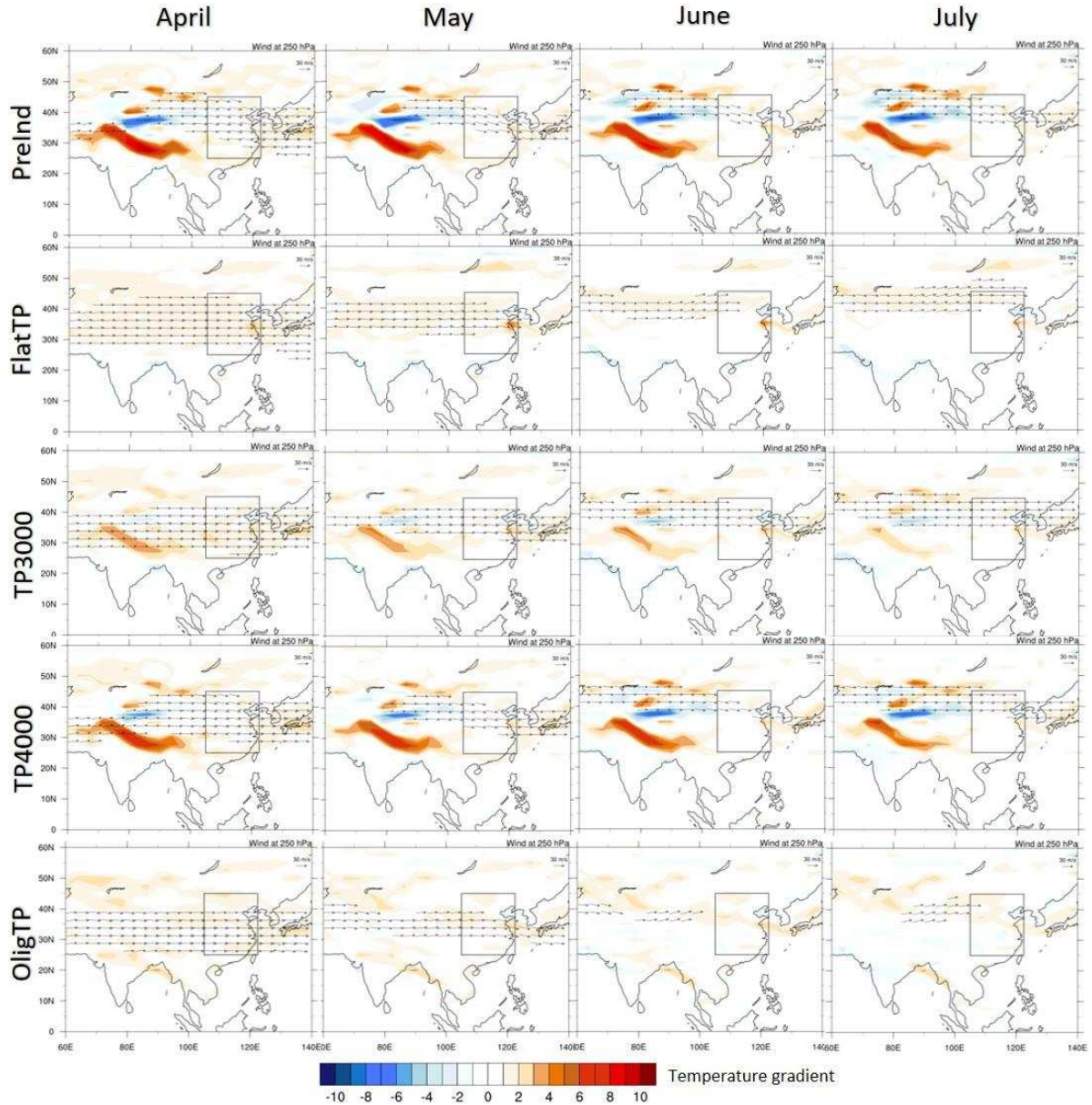
In simulations with elevation higher than TP3000, the latitudinal position of the westerly jet follows the modern-day seasonal variation (Fig. 3). In April the jet over the EAM region is located at 34°N, during May it shifts northward by 2 degrees, in June the jet migrates to the north of the TP and finally, during July the jet acquires its northernmost latitudinal position further north from the TP. However, simulations with lower elevation show a different pattern. Specifically, in experiments FlatTP to experiment TP2000, the westerly jet latitudinal position shifts northwards by only 2° from April to July and does not propagate into the higher latitudes (Fig.3), as the westerlies are not impeded by the TP, and temperature gradient is not as strong with the absence of high elevation over Central Asia (Fig. 4, S2). The four jumps in the westerly jet latitudinal position are also evident in the OligTP experiment. However, due to the difference in the latitudinal distribution of the TP elevation the westerly jet does not reach as far north compared to the PreInd, with its northernmost position being at 40°N (Fig.3).



187

188

189 Fig. 3: Map plots show a schematic of the latitudinal position of the westerly jet (horizontal lines) for months April – July,  
 190 over the EAM region (green box) for each experiment. PreInd (black), FlatTP (blue), TP3000 (magenta), TP4000 (yellow),  
 191 OligTP (red). The integrated graph plots show the latitudinal propagation and windspeed of the low-level southerlies/south-  
 192 easterlies averaged over the EAM region. Notably, the northward propagation of the low-level southerlies/south-easterlies  
 193 is controlled by the latitudinal position of the westerly jet. Experiments TP1000, TP2000 and TP5000 are not shown, as their  
 194 results are similar to the FlatTP for the first two and the PreInd for the latter. The westerly jet position (or jet occurrence) is  
 195 defined at a location where the wind speed is a local maximum (exceeding 30 m/s) between 100 and 500 hPa (Chiang et al.  
 196 2014; Schiemann et al. 2009). The propagation of the low-level winds is given by the position in which the directionality  
 197 changes from south/south-east to westerlies



198

199 Fig. 4: Meridional surface temperature gradient (°C) April – July and 250hPa winds (m/s). Westerlies with speed less than 30  
 200 m/s, which is the lower threshold for a jet occurrence, are masked out. The meridional gradient is defined as  $dT/dLat$ .

201

202 **3.3 850 hPa winds and moisture availability**

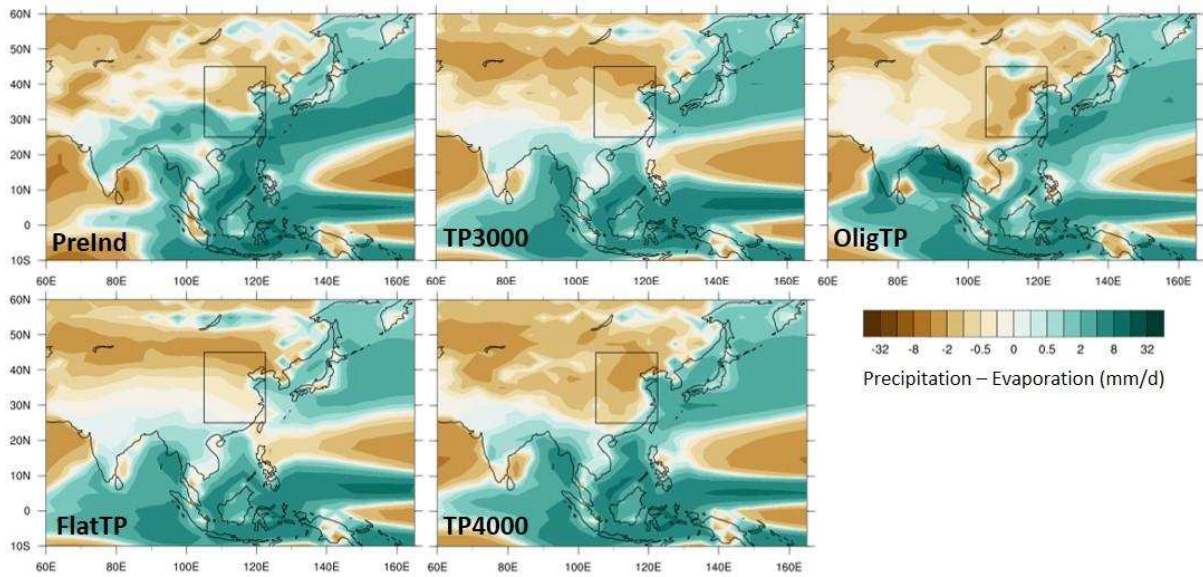
203 It has been well established by previous studies that changes in the elevation of the TP cause a change  
 204 in wind circulation over Asia, not only in the upper troposphere but in the lower as well. In both PreInd  
 205 and TP4000 experiments, easterlies and south-easterlies are dominating the South of the EAM region  
 206 carrying moisture from the Pacific Ocean and South China Sea during April and May and reach higher

207 latitudes during June and July (Fig.3, 5). Spatially, the change from moisture carrying easterlies to  
208 westerlies occurs in the latitude the westerly jet is positioned (Fig. 3).

209 Flattening of the TP, TS and MP, creates a dry zonal area over Asia stretching west to east during  
210 monsoonal months (Fig. 5, S3). In these scenarios the westerlies dominate more than 2/3 of the EAM  
211 region. With the orography flattened completely, the easterlies and south-easterlies do not propagate  
212 to the north, and thus do not contribute as a moisture source for spring precipitation over EAM (Fig.2).

213 Increasing the elevation (TP1000 and TP2000 simulations), leads to a northward propagation of the  
214 westerly jet of about  $2^{\circ}$ , and now the easterlies and south-easterlies propagate into higher latitudes,  
215 but with topography significantly lower than PreInd, moisture availability remains low over the whole  
216 EAM and thus not producing spring precipitation (Fig. 3, 5, S1-3). In TP3000, the westerly jet reaches  
217 its northernmost position, while easterlies and south-easterlies propagate into the EAM region  
218 providing enhanced moisture available in the South. With higher topography over Asia, the pattern of  
219 moisture availability changes from being zonal (running west to east) to a more complex pattern with  
220 the south EAM region's moisture availability increasing (Fig. 3, 5). In TP4000 the simulated wind,  
221 precipitation, humidity and moisture availability begin to display a pattern that is very similar to the  
222 PreInd, and when moving to TP5000 the pattern becomes almost identical to the PreInd (Fig, 2, 3, 5).  
223 In the OligTP experiment the TP is located further South, and the westerlies are significantly weaker  
224 than in any other experiment. However, there moisture is available in the north and northwest of the  
225 EAM to be carried by the westerlies to the north of the EAM. The underlying mechanisms that control  
226 the westerly jet's latitudinal position which in turn controls the EAM precipitation are analysed in  
227 detail by Chiang et al. (2014).

228



229

230 Fig. 5: Moisture availability ( $P - E$ : mm/day) averaged from April to July for different experiments. For elevations less than  
 231 TP3000, broad arid belts are simulated in Asia from West to East, a pattern that changes with higher elevation (TP3000 and  
 232 above).

#### 233 4. Discussion

234 The TP has a marked effect on the westerlies over Asia (Schiemann et al., 2009) and the seasonal  
 235 migration of the westerly jet from South to North is vital to the East Asian rainfall climate (Liang and  
 236 Wang 1998). The “Jet Transition Hypothesis” (Chiang et al. 2014) suggests that changes to the position  
 237 of the westerlies relative to the TP, drive rainfall changes over East Asia over geological timescales.  
 238 Our simulations provide further evidence that the westerly jet transition plays an important role for  
 239 the dynamics of the EAM by controlling the associated monsoonal precipitation. The northward jumps  
 240 of the westerly jet coincide with the stepwise northward propagation of the EAM rainfall during  
 241 monsoonal months (April to July). The westerly jet latitudinal position controls the low-level inland  
 242 flow of moisture-carrying southerlies and south-easterlies over East Asia that leads to precipitation  
 243 where they converge. The lower-level southerly flow is an important factor in the spatial extent and  
 244 seasonality of the EAM (Rodwell and Hoskins 2001). There have been numerous studies deciphering  
 245 the dynamics of the westerly jet and its association to the EAM climate as well as the role of the  
 246 thermal and mechanical forcings from the TP (i.e. Baker et al. 2015; Chiang et al. 2015; Zhang et al.

247 2017, 2018), and it has been established that the high elevation over Asia alters the westerly flow,  
248 which in turn alters the EAM circulation pattern.

249 For elevations greater than TP3000, the pattern of atmospheric circulation is similar to the modern,  
250 with spring precipitation in the southern part of the region controlled by the moisture-carrying  
251 southerlies from the South China Sea and Pacific Ocean. This is consistent with the moisture source  
252 analysis by Baker et al. (2015). However, the EAM does not display the same characteristics when  
253 elevation is less than in experiment TP3000. Notably, with lower elevation the model simulates a  
254 change in monsoonal pattern; specifically, the absence of the first two stages of the present-day  
255 monsoon. With the westerlies flowing zonally and dominating the mid-latitudes over Central Asia,  
256 rather than splitting in the Southern and Northern branch, there is no persistent spring precipitation  
257 (stage 1) and pre-Meiyu phase (stage 2), but there is summer precipitation over the EAM reaching to  
258 the Northern part of the region (albeit weaker and spatially constrained (stages 3 and 4)). In terms of  
259 general precipitation pattern, our simulations are consistent with earlier studies that show that the  
260 uplift of the TP enhances precipitation over East Asia (Jiang et al. 2008; Zhang et al. 2007). The tipping  
261 point for the development of a modern-like circulation is seen in TP3000. This threshold is also  
262 consistent with the simulated shift from zonal arid belts to a non-zonal pattern (Fig. 5), a shift that has  
263 been suggested as an indicator for the onset of the EAM (Li et al. 2018).

264 Even though the land-sea thermal contrast has been suggested in the past as the necessary condition  
265 for spring rainfall over the South EAM region (Tian and Yasunari 1998), Wu et al. (2007) showed that  
266 the spring rainfall is formed when westerlies are split by the TP into a southern and northern branch,  
267 and cold air from the North and warm moist air from the South converge over eastern China. As shown  
268 by our simulations, the deflection of the westerlies, and the subsequent precipitation, occurs when  
269 the TP topography reaches the elevation equivalent to that used within experiment TP3000,  
270 suggesting that with elevations lower than this the EAM misses one of its most characteristic features  
271 - the spring rainfall.



272 Furthermore, the latitudinal position of high elevation is also an important factor that should be taken  
273 into consideration. Our OligTP experiment shows that with elevation closer to the TP2000 but  
274 positioned further to the South, monsoonal circulation is more similar to the PreInd than in the TP2000  
275 experiment, a fact that highlights the importance and necessity for enhanced constraints on the  
276 palaeogeographical history of the region to inform the boundary conditions used for climate modelling  
277 studies.

278 Moving forward, it will be important to study the EAM pattern in a fully palaeoclimate context, using  
279 fully realistic palaeogeographic boundary conditions that not only represent the bulk uplift that  
280 occurred in the region, but also the timing and magnitude of differential uplift of the individual regions  
281 that comprise the TP, TS and MP orogens. This is likely to provide a valuable dataset for proxy data  
282 interpretation. Insights from proxy data in the region are not limited to the intensity and/or the  
283 presence of monsoonal circulation, but also its spatial limits, seasonal variability and monsoonal  
284 phases, and fully realistic palaeo-simulations of the uplift history of the region would prove useful in  
285 terms of interpreting the palaeoclimate signals recorded in different proxy archives.

286 Further work using different climate models with and without realistic palaeogeographic  
287 reconstructions of the region will be necessary to evaluate the model dependency of the elevation  
288 threshold determined in this study for the onset of modern-like circulation in the region.

289

## 290 **5. Conclusions**

291 Using HadCM3, we attempt to determine the effect of the Central Asian orogens uplift to the East  
292 Asian Monsoon (EAM) circulation. Our simulations show that by uplifting the Tibetan Plateau, Tian-  
293 Shan and Mongolian Plateau, there is an evolution towards a modern-like circulation with an elevation  
294 threshold for that change at 3000 m. Lack of high-elevation leads to the westerlies flowing zonally  
295 over Central Asia producing monsoonal precipitation limited to the summer months, whereas when  
296 elevation is set to 3000 m and above, westerlies are deflected by the Tibetan Plateau, and the EAM

297 circulation and associated precipitation follows the pattern seen in the present-day. Furthermore, we  
298 show that the latitudinal position of high elevation is an important factor for the EAM and we highlight  
299 the necessity for constraints on the palaeogeographical boundary conditions that will lead to a better  
300 understanding of the Asian paleoclimate and evolution. Our results show that the latitudinal  
301 distribution of the high elevation can be as important as the uplift in controlling the westerly jet,  
302 seasonal variability and monsoonal precipitation. This factor should be explored through a set of  
303 realistic palaeo-simulations as it has the potential to provide a highly valuable methodology for  
304 interpreting different proxy records.

305

### 306 **Acknowledgments**

307 This work was funded by the Strategic Priority Research Program of the Chinese Academy of Sciences  
308 (XDB26020401) and the National Natural Science Foundation of China (41472151).

309

### 310 **References**

311 Aitken, Alan R.A. 2011. "Did the Growth of Tibetan Topography Control the Locus and Evolution of  
312 Tien Shan Mountain Building?" *Geology* 39(5): 459–62.

313 An, Zhisheng, John E. Kutzbach, Warren L. Prell, and Stephen C. Porter. 2001. "Evolution of Asian  
314 Monsoons and Phased Uplift of the Himalaya-Tibetan Plateau since Late Miocene Times."  
315 *Nature* 411: 62–66. [www.nature.com](http://www.nature.com).

316 Baker, Alexander J. et al. 2015. "Seasonality of Westerly Moisture Transport in the East Asian  
317 Summer Monsoon and Its Implications for Interpreting Precipitation  $\Delta 18O$ ." *Journal of*  
318 *Geophysical Research* 120: 5850–62.

319 Brunet, Marie Françoise, Edward R. Sobel, and Tom Mccann. 2017. "Geological Evolution of Central  
320 Asian Basins and the Western Tien Shan Range." In *Geological Society Special Publication*,

321 Geological Society of London, 1–17.

322 Chiang, John C.H. et al. 2014. “Role of Seasonal Transitions and Westerly Jets in East Asian  
323 Paleoclimate.” *Quaternary Science Reviews* 108: 111–29.

324 Cox, P. M. et al. 1999. “The Impact of New Land Surface Physics on the GCM Simulation of Climate  
325 and Climate Sensitivity.” *Climate Dynamics* 15: 183–203.

326 Dabang, Jiang, Wang Huijun, and Lang Xianmei. 2005. “Evaluation of East Asian Climatology as  
327 Simulated by Seven Coupled Models.” *Advances in Atmospheric Sciences* 22(4): 479–95.

328 Gordon, C. et al. 2000. “The Simulation of SST, Sea Ice Extents and Ocean Heat Transports in a  
329 Version of the Hadley Centre Coupled Model without Flux Adjustments.” *Climate Dynamics* 16:  
330 147–68.

331 De Grave, Johan, Michael M. Buslov, and Peter Van den haute. 2007. “Distant Effects of India–  
332 Eurasia Convergence and Mesozoic Intracontinental Deformation in Central Asia: Constraints  
333 from Apatite Fission-Track Thermochronology.” *Journal of Asian Earth Sciences* 29(2–3): 188–  
334 204. <https://www.sciencedirect.com/science/article/pii/S136791200600071X#!> (September 1,  
335 2019).

336 Gregory, D, G J Shutts, and J R Mitchell. 1998. “A New Gravity-Wave-Drag Scheme Incorporating  
337 Anisotropic Orography and Low-Level Wave Breaking: Impact upon the Climate of the UK  
338 Meteorological Office Unified Model.” *Quarterly Journal of the Royal Meteorological Society*  
339 124(546): 463–93. <https://doi.org/10.1002/qj.49712454606>.

340 Guo, Z. T. et al. 2002. “Onset of Asian Desertification by 22 Myr Ago Inferred from Loess Deposits in  
341 China.” *Nature* 416(6877): 159–63.

342 Jiang, Dabang, Zhongli Ding, Helge Drange, and Yongqi Gao. 2008. “Sensitivity of East Asian Climate  
343 to the Progressive Uplift and Expansion of the Tibetan Plateau under the Mid-Pliocene  
344 Boundary Conditions.” *Advances in Atmospheric Sciences* 25: 709–22.

345 Jolivet, Marc et al. 2007. "Mongolian Summits: An Uplifted, Flat, Old but Still Preserved Erosion  
346 Surface." *Geology* 35(10): 871–74. <https://doi.org/10.1130/G23758A.1>.

347 Lee, Shih Yu, John C.H. Chiang, and Ping Chang. 2015. "Tropical Pacific Response to Continental Ice  
348 Sheet Topography." *Climate Dynamics* 44: 2429–46.

349 Li, Xiangyu, Ran Zhang, Zhongshi Zhang, and Qing Yan. 2018. "Do Climate Simulations Support the  
350 Existence of East Asian Monsoon Climate in the Late Eocene?" *Palaeogeography,*  
351 *Palaeoclimatology, Palaeoecology* 509: 47–57.

352 Liang, Xin Zhong, and Wei Chyung Wang. 1998. "Associations between China Monsoon Rainfall and  
353 Tropospheric Jets." *Quarterly Journal of the Royal Meteorological Society* 124(552): 2597–2623.

354 Lippert, P. C., D. J. J. van Hinsbergen, and G. Dupont-Nivet. 2014. "Early Cretaceous to Present  
355 Latitude of the Central Proto-Tibetan Plateau: A Paleomagnetic Synthesis with Implications for  
356 Cenozoic Tectonics, Paleogeography, and Climate of Asia." *The Geological Society of America*  
357 *Special pa*: 1–29.

358 Liu, Xiao Dong, and Bu Wen Dong. 2013. "Influence of the Tibetan Plateau Uplift on the Asian  
359 Monsoon-Arid Environment Evolution." *Chinese Science Bulletin* 58(34): 4277–91.

360 Liu, Xiaodong et al. 2015. "Impacts of Uplift of Northern Tibetan Plateau and Formation of Asian  
361 Inland Deserts on Regional Climate and Environment." *Quaternary Science Reviews* 116: 1–14.

362 Liu, Xiaodong, and Zhi-Yong Yin. 2002. "Sensitivity of East Asian Monsoon Climate to the Uplift of the  
363 Tibetan Plateau." *Palaeogeography, Palaeoclimatology, Palaeoecology* 183: 223–45.  
364 [www.elsevier.com/locate/palaeo](http://www.elsevier.com/locate/palaeo).

365 Manabe, Syukuro, and Theodore B Terpstra. 1974. "The Effects of Mountains on the General  
366 Circulation of the Atmosphere as Identified by Numerical Experiments." *Journal of the*  
367 *Atmospheric Sciences* 31(1): 3–42. [https://doi.org/10.1175/1520-](https://doi.org/10.1175/1520-0469(1974)031%3C0003:TEOMOT%3E2.0.CO)  
368 [0469\(1974\)031%3C0003:TEOMOT%3E2.0.CO](https://doi.org/10.1175/1520-0469(1974)031%3C0003:TEOMOT%3E2.0.CO).

369 Markwick, Paul J. 2007. "The Palaeogeographic and Palaeoclimatic Significance of Climate Proxies for  
370 Data-Model Comparisons." *Deep-Time Perspectives on Climate Change: Marrying the Signal*  
371 *from Computer Models and Biological Proxies*: 251–312.

372 Molnar, Peter, William R. Boos, and David S. Battisti. 2010a. "Orographic Controls on Climate and  
373 Paleoclimate of Asia: Thermal and Mechanical Roles for the Tibetan Plateau." *Annual Review of*  
374 *Earth and Planetary Sciences* 38: 77–102.

375 Pope, V. D., M. L. Gallani, P. R. Rowntree, and R. A. Stratton. 2000. "The Impact of New Physical  
376 Parametrizations in the Hadley Centre Climate Model: HadAM3." *Climate Dynamics* 16(2–3):  
377 123–46.

378 Pope, V D, J A Pamment, D R Jackson, and A Slingo. 2001. "The Representation of Water Vapor and  
379 Its Dependence on Vertical Resolution in the Hadley Centre Climate Model." *Journal of Climate*  
380 14(14): 3065–85. [https://doi.org/10.1175/1520-0442\(2001\)014%3C3065:TROWVA%3E2.0.CO](https://doi.org/10.1175/1520-0442(2001)014%3C3065:TROWVA%3E2.0.CO).

381 Rodwell, M J, and B J Hoskins. 2001. "Subtropical Anticyclones and Summer Monsoons." *Journal of*  
382 *Climate* 14(15): 3192–3211. [https://doi.org/10.1175/1520-](https://doi.org/10.1175/1520-0442(2001)014%3C3192:SAASM%3E2.0.CO)  
383 [0442\(2001\)014%3C3192:SAASM%3E2.0.CO](https://doi.org/10.1175/1520-0442(2001)014%3C3192:SAASM%3E2.0.CO).

384 Rowley, David B., and Brian S. Currie. 2006. "Palaeo-Altometry of the Late Eocene to Miocene  
385 Lunpola Basin, Central Tibet." *Nature* 439: 677–81.

386 Schiemann, Reinhard, Daniel Lüthi, and Christoph Schär. 2009. "Seasonality and Interannual  
387 Variability of the Westerley Jet in the Tibetan Plateau Region." *Journal of Climate* 22: 2940–57.

388 Smith, R N B. 1990. "A Scheme for Predicting Layer Clouds and Their Water Content in a General  
389 Circulation Model." *Quarterly Journal of the Royal Meteorological Society* 116(492): 435–60.  
390 <https://doi.org/10.1002/qj.49711649210>.

391 Sobel, Edward R., and Trevor A. Dumitru. 1997. "Thrusting and Exhumation around the Margins of  
392 the Western Tarim Basin during the India-Asia Collision." *Journal of Geophysical Research: Solid*

393 *Earth* 102(B3): 5043–63.

394 Tian, S.-F, and Tetsuzo Yasunari. 1998. “Climatological Aspects and Mechanism of Spring Persistent  
395 Rains over Central China.” *Journal of the Meteorological Society of Japan* 76: 57–70.

396 Windley, Brian F, and Mark B Allen. 1993. “Mongolian Plateau: Evidence for a Late Cenozoic Mantle  
397 Plume under Central Asia.” *Geology* 21(4): 295–98. [https://doi.org/10.1130/0091-](https://doi.org/10.1130/0091-7613(1993)021%3C0295:MPEFAL%3E2.3.CO)  
398 [7613\(1993\)021%3C0295:MPEFAL%3E2.3.CO](https://doi.org/10.1130/0091-7613(1993)021%3C0295:MPEFAL%3E2.3.CO).

399 Wu, Guoxiong et al. 2007. “The Influence of Mechanical and Thermal Forcing by the Tibetan Plateau  
400 on Asian Climate.” *Journal of Hydrometeorology* 8: 770–89.

401 Yin, A. et al. 1998. “Late Cenozoic Tectonic Evolution of the Southern Chinese Tian Shan.” *Tectonics*  
402 17: 1–27.

403 Zhang, Qiong et al. 2007. “The Influence of Mechanical and Thermal Forcing by the Tibetan Plateau  
404 on Asian Climate.” *Journal of Hydrometeorology* 8: 770–89.

405 Zhang, Ran et al. 2017. “Comparison of the Climate Effects of Surface Uplifts from the Northern  
406 Tibetan Plateau, the Tianshan, and the Mongolian Plateau on the East Asian Climate.” *Journal*  
407 *of Geophysical Research* 122: 7949–70.

408 ———. 2018. “Changes in Tibetan Plateau Latitude as an Important Factor for Understanding East  
409 Asian Climate since the Eocene: A Modeling Study.” *Earth and Planetary Science Letters*.

410 Zoura, D. et al. 2019. “Atmospheric Carbon Dioxide, Ice Sheet and Topographic Constraints on  
411 Palaeo Moisture Availability in Asia.” *Earth and Planetary Science Letters* 519: 12–27.

412